Finite-Difference Analysis of Dispersive Transmission Lines Within a Circuit Simulator

Behzad Kordi, Joe LoVetri, *Member, IEEE*, and Greg E. Bridges, *Senior Member, IEEE*

***Abstract*—In this paper, a finite-difference time-domain (FDTD) analysis of the transmission line equations for a general circuit simulator is presented. A two-port circuit representation is derived for integrating a dispersive transmission line network within a circuit/system simulator. The circuit model consists of resistive elements and dependent current sources, which are updated at every time step by the FDTD algorithm. The frequency dependence of the conductors' parameters is taken care of by a recursive integration that employs the Vector Fitting algorithm. The application of this model is presented for several examples, such as nonuniform transmission lines, plane wave excitation of the line, and determination of overvoltages induced by a nearby lightning stroke.**

***Index Terms*—Distributed parameter circuits, electromagnetic coupling, FDTD methods, frequency-dependent parameters, lightning, time-frequency analysis, transmission line model.**

I. Introduction

MULTICONDUCTOR transmission lines (MTLs) arise in applications ranging from very long over-head lines and cables in power transmission to tiny interconnects in VLSI technology and electronic chip packaging. Accurate and efficient simulation is important for all these applications. A fundamental difficulty encountered in integrating transmission-line simulation into a transient circuit simulator arises because network nonlinearities and/or time-dependent components require a time domain analysis, whereas transmission line characteristics such as conductor loss and dispersion are best described in the frequency domain. The issue of mixed time-frequency modeling of lossy coupled multiconductor transmission lines has been studied in both the power systems and the electronics communities for many years.

Many researchers have studied the problem of simulating dispersive transmission lines in the time domain. One of the first models, referred to as the method of characteristics, can only deal with lossless transmission lines. This simple delay model was considered by Branin [1]. The issue of modeling transmission lines with frequency-dependent parameters, which has emerged as an important topic in the power systems area, was studied by Budner [2]. He considered a modal analysis and included the frequency-dependence of the line parameters using a convolution of the past history of the modal voltages and weighting functions where the weighting functions are the inverse transform of the two-port admittance parameters. Only symmetric transmission lines were studied, which, however, result in a frequency-independent transformation matrix. Because of the high computational cost of evaluating the convolution integrals in Budner's model, a more efficient model was proposed by Snelson [3], which is formulated using forward and backward traveling waves. Improving Budner's weighting functions, and modifying the method proposed by Snelson, Marti developed an equivalent circuit impedance model, which is an approximation to the frequency-dependent characteristic impedance of the line [4]. His model employs modal analysis with a frequency-independent transformation matrix and is the progenitor of common models employed in power system simulators (such as PSCAD [5] and EMTP [6]). One of the disadvantages of this model is its poor accuracy in simulating low-frequency coupling effects [7]. This deficiency is overcome by including the frequency variation of the transformation matrix in the simulation [8]. In [8], the same fitting algorithms as those formulated in [4] were used for underground cables, where accounting for the frequency dependence is essential. In general, however, this approach is not guaranteed to be stable in the case of overhead transmission lines [9]. To avoid the inaccuracy or instability problems observed in the mode-domain models, a variety of methods in which the matrix elements of the propagation function and the characteristic admittance are directly studied and fitted in the phase domain, have been proposed (see, for example, [10]–[13]). A review of phase domain models can be found in the work of Gustavsen *et al.* [7].

Finite-difference time-domain (FDTD) methods are a common way of approximating the time-domain response of transmission lines [14], [15]. The MTL equations are discretized both in time and space and the resulting difference equations are usually solved using the leap-frog scheme [16]. Basic FDTD approaches have been applied to problems with frequency-independent per-unit-length parameters. The inclusion of terminal constraints [17], lossy conductors [18], and nonlinear junctions [19] have been addressed. The main problem with interfacing circuit-simulator nodes to the solution of the MTL equations is that in the standard leap-frog FDTD implementation, the discretized line voltages and currents are not collocated in space and time, whereas the circuit-simulator nodal voltages and currents are collocated in both space and time. In [17], a first-order finite-difference approximation for one of the MTL equations was proposed to relate terminal voltages and currents, and a state-variable formulation was used to solve the whole MTL network. The skin-effect frequency dependence of the transmission-line conductors was considered in [18], where the series transmission line impedance

Manuscript received June 2, 2004; revised November 5, 2004. This work was supported by Manitoba Hydro, Manitoba, Canada. Paper no. TPWRD-00264-2004.

The authors are with the Department of Electrical and Computer Engineering, University of Manitoba, Winnipeg, MB, Canada R3T 5V6 (e-mail: bkordi@ee.umanitoba.ca; lovetri@ee.umanitoba.ca; bridges@ee.umanitoba.ca).

Digital Object Identifier 10.1109/TPWRD.2005.855431

was approximated by a rational function. A technique for incorporating the FDTD formulation in a lumped-element network simulator using modified nodal analysis (MNA) was introduced by Mardare and LoVetri [19]. They only considered frequency-independent lines.

In this paper, we present a novel technique for the inclusion of an FDTD formulation capable of modeling dispersive frequency-dependent transmission lines within a circuit/system simulator. In this method, the transmission line is represented as a two-port stamp, which includes dependent current sources. The current sources are updated at each time step by the FDTD algorithm. The two-port stamp contains resistive elements only, which makes the model independent from the scheme used by the simulator for approximating derivatives. Using the Vector Fitting algorithm [20], we have developed an accurate recursive approximation for the convolution integrals needed for modeling the frequency dependence of the line parameters. In this paper, we have chosen PSCAD/EMTDC as the simulation environment, even though the approach is applicable to other simulators.

Details of the FDTD formulation, which include the frequency-dependence of the MTL equations and the method of including the terminal constraints, are given. We also give details of including the coupling of an external field to the transmission line: specifically, the fields associated with a plane wave or a lightning discharge. In order to verify the accuracy of the method we compare results with a frequency-domain solution. We also show the method's ability to model nonuniform transmission lines by considering the example of a power transmission line over a terrain with varying electrical parameters.

II. FDTD Formulation

FDTD methods are commonly used for numerical solution of partial differential equations in electromagnetics [21], as well as MTL equations [16]. The derivatives in the MTL equations can be discretized and approximated with various finite differences schemes. We chose an explicit time-space second-order central finite-difference scheme, similar to that described by Paul [16]. In this section, the discretization of the MTL equations is presented first, and then the generation of a link between the variables in the FDTD model of the line and the terminal variables is presented.

A. FDTD Discretization of MTL Equations

Consider an $(N+1)$-conductor uniform transmission line, as shown in Fig. 1. The general MTL equations in the Laplace domain are

$$\frac{\partial}{\partial x}\mathbf{I}(x,s)+\mathbf{Y}(s)\mathbf{V}(x,s)=\mathbf{0} \tag{1a}$$

$$\frac{\partial}{\partial x}\mathbf{V}(x,s)+\mathbf{Z}(s)\mathbf{I}(x,s)=\mathbf{0} \tag{1b}$$

where $\mathbf{V}(x,s)$ and $\mathbf{I}(x,s)$ are N-vectors of the line voltage and current, respectively. Matrices $\mathbf{Y}(s)$ and $\mathbf{Z}(s)$ represent the line shunt admittance and series impedance matrices, respectively. The space variable is x and s is the Laplace variable.

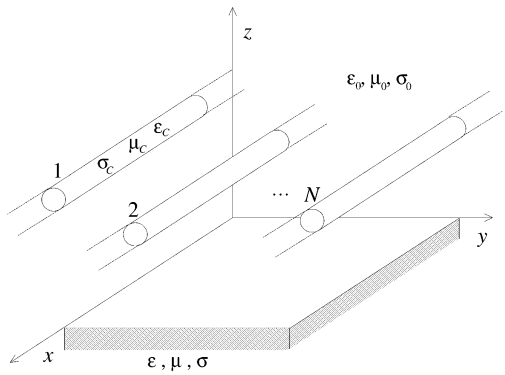

Fig. 1. Geometry of the multiconductor transmission line over a lossy ground.

Assuming the conductors are insulated from the surrounding medium with a lossy dielectric that is frequency independent, the shunt admittance can be modeled as a simple shunt capacitance and conductance. On the other hand, the series impedance can show strong frequency-dependence due to both the ground and the conductors losses. This is modeled as

$$\mathbf{Y}(s)=\mathbf{G}+s\mathbf{C} \tag{2a}$$

$$\mathbf{Z}(s)=\mathbf{R}+s\mathbf{L}+\mathbf{Z}'(s) \tag{2b}$$

$$\mathbf{Z}'(s)=\sum_{i=1}^{M}\frac{\mathbf{a}_i}{s-\alpha_i} \tag{2c}$$

where the frequency dependence of the series impedance has been taken into account using $\mathbf{Z}'(s)$. In (2a), $\mathbf{G}$ and $\mathbf{C}$ are the frequency-independent per-unit-length conductance and capacitance matrices, whereas $\mathbf{R}$, $\mathbf{L}$, and $\mathbf{Z}'(s)$, in (2b), are determined by using the Vector Fitting algorithm [20]. This algorithm fits $\mathbf{Z}(s)$ using a sum of M first-order poles α_i with corresponding residues $\mathbf{a}_i$, a proportional term $s\mathbf{L}$, and a constant term $\mathbf{R}$. For the overhead line cases considered in this paper, $\mathbf{Z}(s)$ is initially determined using the physical parameters and Carson's formulation [22].

For ease of exposition and without loss of generality, the FDTD discretization scheme is described as applied to a single-conductor transmission line. The extension of the formulation to multiconductor transmission lines is straightforward. This is an inherent advantage of this technique, whereas other methods are often difficult to extend to the multiconductor case.

Using (2), we now write (1) in the time domain as

$$\frac{\partial}{\partial x}I(x,t)+C\frac{\partial}{\partial t}V(x,t)+GV(x,t)=0 \tag{3a}$$

$$\frac{\partial}{\partial x}V(x,t)+L\frac{\partial}{\partial t}I(x,t)+RI(x,t)+Z'(t)*I(x,t)=0 \tag{3b}$$

where, in (3b), $*$ represents the convolution operator. Usually, the convolution term is employed directly in the form given in (3b). In order to calculate the convolution integral more accurately we introduce the following modification

$$Z'(s)I(x,s)=\frac{Z'(s)}{s}\cdot sI(x,s). \tag{4}$$

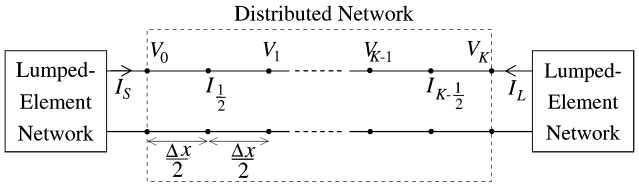

Fig. 2. Interlaced voltages and currents of the FDTD approximation of a transmission line that is connected to networks with lumped elements. Despite the lines voltages and currents, the terminal voltages and currents are both collocated in time and space.

This means that, instead of convolving $Z'(t)$ with the current, we convolve the integral of $Z'(t)$ with the time-domain derivative of the current:

$$Z'(t) * I(x,t) = \int_0^t Z'(\tau)d\tau * \frac{\partial}{\partial t} I(x,t) \tag{5a}$$

$$\int_0^t Z'(\tau)d\tau = \sum_{i=1}^{M} \frac{a_i}{\alpha_i}(e^{\alpha_i t} - 1) = \sum_{i=1}^{M} \frac{a_i}{\alpha_i} e^{\alpha_i t} - \sum_{i=1}^{M} \frac{a_i}{\alpha_i}. \tag{5b}$$

The advantage of this approach is discussed later.

Using (5), we can rewrite (3b) as

$$\frac{\partial}{\partial x} V(x,t) + L\frac{\partial}{\partial t} I(x,t) + (R - \Gamma) I(x,t) + \Phi(t) * \frac{\partial}{\partial t} I(x,t) = 0 \tag{6a}$$

where

$$\Gamma = \sum_{i=1}^{M} \frac{a_i}{\alpha_i} \tag{6b}$$

$$\Phi(t) = \sum_{i=1}^{M} \frac{a_i}{\alpha_i} e^{\alpha_i t}. \tag{6c}$$

An FDTD model is developed by discretizing (3a) and (6a). We divide the line into K spatial segments each of length Δx, and consider the time step to be Δt. In order to ensure the stability of the discretization and second-order accuracy of the scheme, the voltages and currents are interlaced both in time and space. As shown in Fig. 2, voltage and adjacent current points are separated by $\Delta x/2$ in space and $\Delta t/2$ in time. This is also true for the terminals, but in order to incorporate the terminal constraints we need to collocate the line voltages and currents at the terminations. The procedure for this will be described later. The second-order central difference approximations to (3a) and (6a) become

$$\frac{I_{k+\frac{1}{2}}^{n+\frac{1}{2}} - I_{k-\frac{1}{2}}^{n+\frac{1}{2}}}{\Delta x} + C\frac{V_k^{n+1} - V_k^n}{\Delta t} + G\frac{V_k^{n+1} + V_k^n}{2} = 0 \tag{7a}$$

$$\frac{V_{k+1}^n - V_k^n}{\Delta x} + L\frac{I_{k+\frac{1}{2}}^{n+\frac{1}{2}} - I_{k+\frac{1}{2}}^{n-\frac{1}{2}}}{\Delta t} + (R - \Gamma)\frac{I_{k+\frac{1}{2}}^{n+\frac{1}{2}} + I_{k+\frac{1}{2}}^{n-\frac{1}{2}}}{2} + \int_0^{n\Delta t} \Phi(\tau)\frac{\partial}{\partial(n\Delta t - \tau)} I_{k+\frac{1}{2}}(n\Delta t - \tau)d\tau = 0. \tag{7b}$$

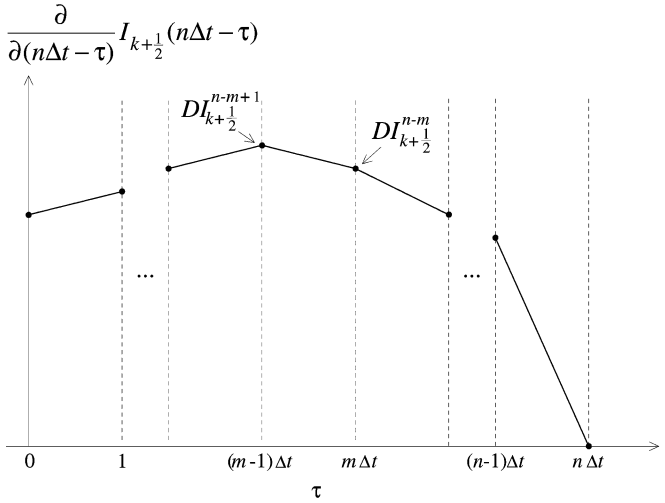

Fig. 3. Piece-wise-linear approximation for the mirrored and shifted current derivative. The data points of this curve are denoted as $DI_{k+(1/2)}$.

In (7), k and n are space and time indices, respectively. Solving (7b) for $I_{k+(1/2)}^{n+(1/2)}$ and (7a) for V_k^{n+1}, we obtain the update equations. However, in order to make the algorithm time and memory efficient, the convolution term in (7b) should be calculated recursively. The recursive approximation we use is discussed next.

B. Recursive Convolution Integral

The idea of recursive integration using exponentials combined with FDTD has been discussed in several papers (for example, [16]–[18]). In [16], the author showed how to include the skin effect into the series impedance of a two-wire line in free space using a $\sqrt{s}$ variation. This was then modeled in the time domain as a sum of exponentials using the Prony's method presented in [23] to obtain a recursive integration scheme. It has been shown, however, that this approximation gives prediction errors that are significant in some classes of problems [24].

In this paper, the exponential approximation, which is obtained by the Vector Fitting method [20], makes the recursive integration possible. To visualize the convolution integral, we assume a typical waveshape for the time derivative of the current at data point $k+(1/2)$. To perform the convolution it has to be mirrored and shifted in time by n time steps (see Fig. 3). Determining the convolution integral in (7b) over segments each of length Δt, we can write

$$\Phi(t) * \frac{\partial}{\partial t} I_{k+\frac{1}{2}}(t) = \sum_{m=1}^{n} \int_{(m-1)\Delta t}^{m\Delta t} \Phi(\tau)\frac{\partial}{\partial(n\Delta t - \tau)} I_{k+\frac{1}{2}}(n\Delta t - \tau)d\tau. \tag{8}$$

In the calculation of (8), we use the half-time-step shift between the voltage and current points to our advantage. Using a central difference approximation for the calculation of the time derivative of (8), the data points of the time derivative of the current are evaluated at integer multiples of the time step, which is similar to the voltage points. A piecewise-linear approximation of the current time derivative in (8) is used over each time step, as shown in Fig. 3. In this figure, the data points of the mirrored

and shifted current derivative are denoted by $DI_{k+(1/2)}$. Using this approximation, we can rewrite (8) as

$$\Phi(t) * \frac{\partial}{\partial t} I_{k+\frac{1}{2}}(t) = \sum_{i=1}^{M} \frac{a_i}{\alpha_i} \sum_{m=1}^{n} \left(A_m \xi_i^m + B_m \chi_i^m\right) \quad (9a)$$

where

$$A_m = 2I_{k+\frac{1}{2}}^{n-m+\frac{1}{2}} - I_{k+\frac{1}{2}}^{n-m-\frac{1}{2}} - I_{k+\frac{1}{2}}^{n-m+\frac{3}{2}} \quad (9b)$$

$$B_m = I_{k+\frac{1}{2}}^{n-m+\frac{1}{2}} - I_{k+\frac{1}{2}}^{n-m-\frac{1}{2}} \quad (9c)$$

$$\xi_i^m = \frac{1}{\Delta t^2} \int_{(m-1)\Delta t}^{m\Delta t} e^{\alpha_i \tau} (\tau - m\Delta t) d\tau \quad (9d)$$

$$\chi_i^m = \frac{1}{\Delta t} \int_{(m-1)\Delta t}^{m\Delta t} e^{\alpha_i \tau} d\tau. \quad (9e)$$

The integrals in (9d) and (9e) can be calculated recursively as

$$\xi_i^m = \frac{e^{\alpha_i (m-1)\Delta t}}{\alpha_i \Delta t} \left(1 + \frac{1}{\alpha_i \Delta t} - \frac{e^{\alpha_i \Delta t}}{\alpha_i \Delta t}\right) \quad (10a)$$

$$\xi_i^m = e^{\alpha_i \Delta t} \xi_i^{m-1} \quad (10b)$$

$$\chi_i^m = \frac{e^{\alpha_i (m-1)\Delta t}}{\alpha_i \Delta t} (e^{\alpha_i \Delta t} - 1) \quad (11a)$$

$$\chi_i^m = e^{\alpha_i \Delta t} \chi_i^{m-1}. \quad (11b)$$

In this way, we do not need to store the whole history of the currents and the computation cost is dramatically reduced.

Finally, the convolution integral (8) can be evaluated as

$$\Phi(t) * \frac{\partial}{\partial t} I_{k+\frac{1}{2}}(t) = \sum_{i=1}^{M} \frac{a_i}{\alpha_i} \left[A_1 \xi_i^1 + B_1 \chi_i^1 + \sum_{m=2}^{n} \left(A_m \xi_i^m + B_m \chi_i^m\right) \right] \quad (12)$$

where, from (9b) and (9c)

$$A_1 = 2I_{k+\frac{1}{2}}^{n-\frac{1}{2}} - I_{k+\frac{1}{2}}^{n-\frac{3}{2}} - I_{k+\frac{1}{2}}^{n+\frac{1}{2}} \quad (13a)$$

$$B_1 = I_{k+\frac{1}{2}}^{n-\frac{1}{2}} - I_{k+\frac{1}{2}}^{n-\frac{3}{2}}. \quad (13b)$$

Identifying the last summation of (12) as

$$\Psi_i^n = \sum_{m=2}^{n} \left(A_m \xi_i^m + B_m \chi_i^m\right) \quad (14)$$

and using (10b) and (11b), one can easily show that

$$\Psi_i^n = \left(2I_{k+\frac{1}{2}}^{n-\frac{3}{2}} - I_{k+\frac{1}{2}}^{n-\frac{5}{2}} - I_{k+\frac{1}{2}}^{n-\frac{1}{2}}\right) \xi_i^2 + \left(I_{k+\frac{1}{2}}^{n-\frac{3}{2}} - I_{k+\frac{1}{2}}^{n-\frac{5}{2}}\right) \chi_i^2 + e^{\alpha_i \Delta t} \Psi_i^{n-1} \quad (15)$$

which requires storage of only Ψ_i^{n-1} and three previous current vectors in order to calculate the integral term in (7b).

C. FDTD Update Equations

The FDTD update equations for $I_{k+(1/2)}^{n+(1/2)}$ and V_k^{n+1} can now be defined. First, (7b) is used to update $I_{k+(1/2)}^{n+(1/2)}$, which is half a time step leading the voltage V_k^{n+1} as

$$I_{k+\frac{1}{2}}^{n+\frac{1}{2}} = \frac{Z_1 I_{k+\frac{1}{2}}^{n-\frac{1}{2}} + \Delta x(\xi + \chi) I_{k+\frac{1}{2}}^{n-\frac{3}{2}} - \left(V_{k+1}^n - V_k^n\right) - \Delta x \Psi^n}{Z_2} \quad (16a)$$

where

$$Z_1 = \Delta x \left(\frac{L}{\Delta t} - \frac{R}{2} + \frac{\Gamma}{2} - 2\xi - \chi\right) \quad (16b)$$

$$Z_2 = \Delta x \left(\frac{L}{\Delta t} + \frac{R}{2} - \frac{\Gamma}{2} - \xi\right) \quad (16c)$$

$$\xi = \sum_{i=1}^{M} \frac{a_i}{\alpha_i} \xi_i^1 \quad (16d)$$

$$\chi = \sum_{i=1}^{M} \frac{a_i}{\alpha_i} \chi_i^1 \quad (16e)$$

$$\Psi^n = \sum_{i=1}^{M} \frac{a_i}{\alpha_i} \Psi_i^n. \quad (16f)$$

Then, (7a) is used to update V_k^{n+1} as

$$V_k^{n+1} = \frac{Y_1 V_k^n - \left(I_{k+\frac{1}{2}}^{n+\frac{1}{2}} - I_{k-\frac{1}{2}}^{n+\frac{1}{2}}\right)}{Y_2} \quad (17a)$$

where

$$Y_1 = \Delta x \left(\frac{C}{\Delta t} - \frac{G}{2}\right) \quad (17b)$$

$$Y_2 = \Delta x \left(\frac{C}{\Delta t} + \frac{G}{2}\right). \quad (17c)$$

It is worth noting that all the parameters involved in (16) and (17) (except for Ψ^n) are not changing with time and need to be calculated only once. Even Ψ^n contains constants that require evaluation only at the beginning of the algorithm. This update scheme is illustrated in Fig. 4. The values of the line voltages at time step n and previous values of the line currents are used to update the line currents at time step $n+(1/2)$, and then the line voltages (except for the terminal voltages) are updated at time step $n+1$. The updating process for the terminal voltages and currents are taken care of by the circuit/system simulator, which is discussed next.

D. Terminal Constraints

The update equations of the FDTD scheme cannot be applied to the terminal voltages. The essential problem in incorporation of the terminal conditions is that the FDTD voltages and currents at each end of the line are not collocated in space or time, whereas the terminal conditions relate the voltage and current at the same position and time (see Fig. 4). The terminal currents, which we denote as I_S and I_L, are collocated in time and space

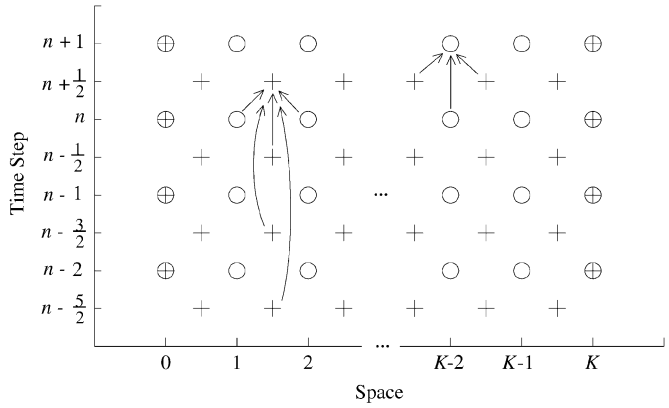

Fig. 4. Time-space distribution of the line voltages (o) and currents (+). At the terminal, the voltage and currents are collocated both in time and space.

with the terminal voltages, V_0 and V_K. At the $k = 0$ terminal, the first MTL equation given in (3a) is discretized at $x = 0$ as [17]

$$\frac{1}{\frac{\Delta x}{2}}\left(I_{\frac{1}{2}}^{n+\frac{1}{2}} - \frac{I_S^{n+1} + I_S^n}{2}\right) + C\frac{V_0^{n+1} - V_0^n}{\Delta t} + G\frac{V_0^{n+1} + V_0^n}{2} = 0. \quad (18)$$

Solving (18) for I_S^{n+1} yields

$$I_S^{n+1} = I_{\mathrm{SH}}^{n,n+\frac{1}{2}} + G_{\mathrm{eq}} V_0^{n+1} \quad (19a)$$

where

$$G_{\mathrm{eq}} = \Delta x\left(\frac{G}{2} + \frac{C}{\Delta t}\right) \quad (19b)$$

$$I_{\mathrm{SH}}^{n,n+\frac{1}{2}} = 2I_{\frac{1}{2}}^{n+\frac{1}{2}} - I_S^n + \Delta x\left(\frac{G}{2} - \frac{C}{\Delta t}\right)V_0^n. \quad (19c)$$

Similarly, (3a) can be discretized at the other terminal to obtain

$$I_L^{n+1} = I_{\mathrm{LH}}^{n,n+\frac{1}{2}} + G_{\mathrm{eq}} V_K^{n+1} \quad (20a)$$

where

$$I_{\mathrm{LH}}^{n,n+\frac{1}{2}} = -2I_{K-\frac{1}{2}}^{n+\frac{1}{2}} - I_L^n + \Delta x\left(\frac{G}{2} - \frac{C}{\Delta t}\right)V_K^n. \quad (20b)$$

Observe that the terminal current at this point is directed into the line in order to provide symmetry of the equivalent circuit. This has been taken into account by the negative sign of the first term on the right-hand side of (20b).

The circuit representation of (19a) and (20a) is demonstrated in Fig. 5. This circuit is composed of resistive elements and dependent current sources that are updated by (19c) and (20b). In each time step, the FDTD algorithm is called by the circuit simulator and the line's internal currents and voltages $I_{k+(1/2)}^{n+(1/2)} k \in \{0, 1, \ldots, K-1\}$ and $V_k^{n+1} k \in \{1, 2, \ldots, K-1\}$ are updated based on their past values and the terminals' voltages past values, V_0^n and V_K^n. Next, the history current sources, I_{SH} and I_{LH}, are updated and their values are passed to the circuit simulator, which then solves the network and updates the terminals' currents and voltages.

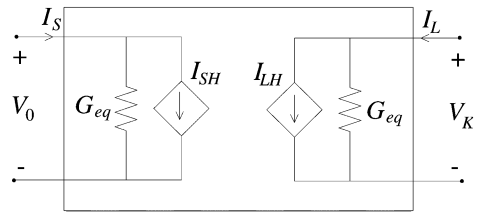

Fig. 5. Two-port stamp for the transmission line circuit model. The FDTD algorithm at each time step updates history current sources I_{SH} and I_{SL}. G_{eq} is determined by the line parameters and the time and the space steps.

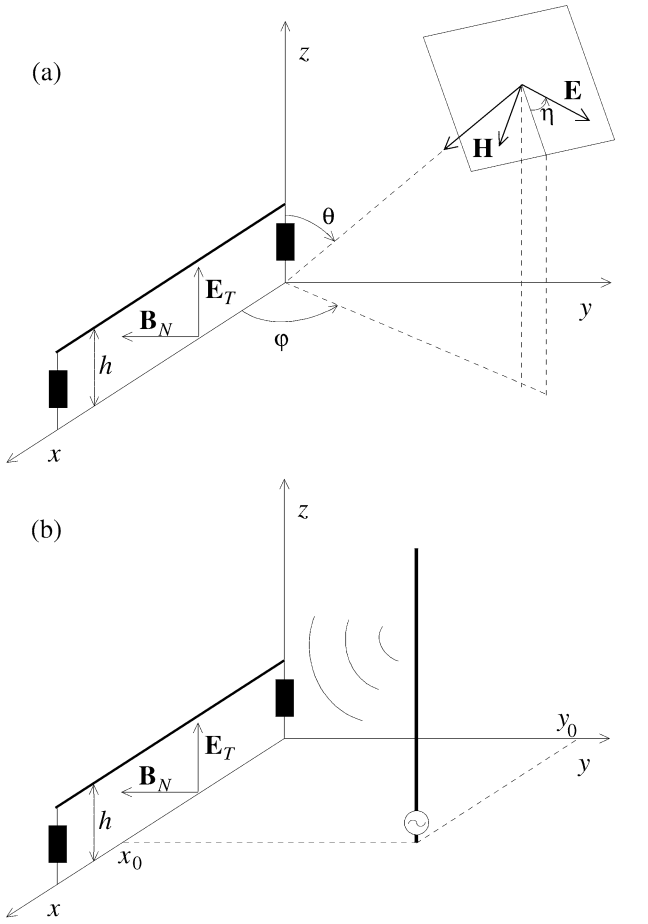

Fig. 6. Example of a transmission line illuminated by (a) a plane wave and (b) the fields generated by a nearby lightning stroke.

E. External Field Coupling

Simulation software based on terminal-characteristic models, such as PSCAD and EMTP, are not capable of calculating external-field coupling, whereas one of the inherent features of distributed models is the capability of determining the response of the line to external exciting fields. The source of such electromagnetic fields can be, for example, a plane wave or a nearby lightning stroke (see Fig. 6). The external fields are introduced into the transmission line equations as voltage and

current sources at the right hand side of the equations. Thereby, (3a) and (3b) are rewritten as [16]

$$\frac{\partial}{\partial x}I(x,t)+C\frac{\partial}{\partial t}V(x,t)+GV(x,t)=I_e(x,t) \quad (21a)$$

$$\frac{\partial}{\partial x}V(x,t)+L\frac{\partial}{\partial t}I(x,t)+RI(x,t) + Z'(t)*I(x,t)=V_e(x,t) \quad (21b)$$

where the exciting current and voltage sources are defined in terms of the transverse electric field and normal magnetic flux density [25]

$$I_e(x,t)=-G\int_0^h E_T(x,z,t)\,dz-C\frac{\partial}{\partial t}\int_0^h E_T(x,z,t)dz \quad (22a)$$

$$V_e(x,t)=\frac{\partial}{\partial t}\int_0^h B_N(x,z,t)\,dz. \quad (22b)$$

In (22), h is the height of the line, and the integration path is along the cross section of the line, from the ground to the conductor.

Note that when applying the discretization scheme of the FDTD approach to the source terms, the sources should also be interlaced both in time and space. Since (21a) and (21b) are expanded at time $n+(1/2)$ and location k and time n and location $k+(1/2)$, respectively, we can write (22) as

$$I_{ek}^{n+\frac{1}{2}}=-h\left(G\frac{E_{Tk}^{n+1}+E_{Tk}^{n}}{2}+C\frac{E_{Tk}^{n+1}-E_{Tk}^{n}}{\Delta t}\right) \quad (23a)$$

$$V_{e\left(k+\frac{1}{2}\right)}^{n}=h\frac{B_{N\left(k+\frac{1}{2}\right)}^{n+\frac{1}{2}}-B_{N\left(k+\frac{1}{2}\right)}^{n-\frac{1}{2}}}{\Delta t}. \quad (23b)$$

In the derivation of (23a) and (23b), we have assumed that the exciting fields are constant along the cross section of the line. Now, for the case of an external-field excitation, the FDTD update equations (16a) and (17a) should be revised, considering the source terms derived in (23).

III. Simulation Results

The FDTD method described in the previous section has the capability of providing access to both the per-unit-length parameters as well as the transmission-line variables along the whole length of the line. This can be used to simulate the effect of distributed external field excitation, for example. The source of such an external electromagnetic field can be a plane wave or a nearby lightning stroke. The method also enables simulation of nonuniform lines for which the per-unit-length parameters are functions of the line's spatial parameter. In this section, four cases are studied. First, a simple single-conductor overhead line with frequency-dependent parameters is simulated. The simplicity of the problem allows us to investigate the capability of the proposed approach for the modeling parameters. A nonuniform line is presented next. Finally, two examples investigating plane wave and lightning-stroke-generated field coupling to transmission lines are presented. All of these results have been generated using PSCAD as the circuit simulation platform. The extension of this method to multiconductor transmission lines is fairly straightforward.

TABLE I
Single-Conductor Line Parameters

Conductor Height	10 m
Conductor Radius	2 cm
Conductor Resistivity	0.5×10^{-6} Ωm
Ground Resistivity	10000 Ωm
Length	10 km

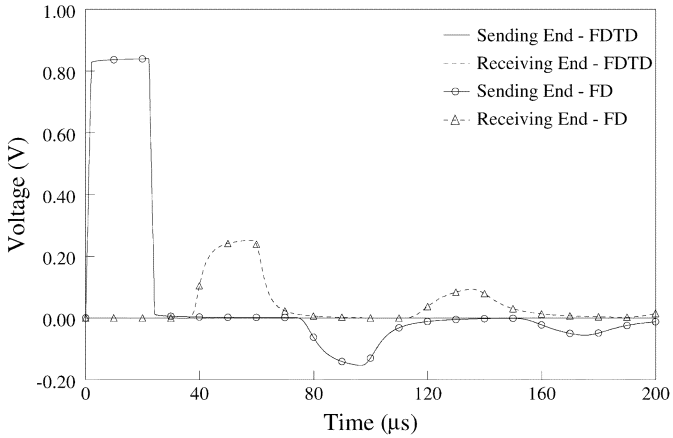

Fig. 7. Terminal voltages of the uniform line when excited by a trapezoidal waveform. FDTD Results are compared to those obtained using a direct frequency-domain (FD) method.

A. Uniform Single-Conductor Transmission Line

To examine the accuracy of the FDTD algorithm, we first consider a single-conductor overhead transmission line whose parameters are given in Table I. The line is excited by a unit-amplitude trapezoidal waveform that has a 22-μs duration and 2-μs rise and fall times and is terminated with 100-Ω loads at both ends. Using the FDTD technique, implemented in the PSCAD environment, the voltages at the two terminals of the line were calculated as shown in Fig. 7. A time step of $\Delta t = 0.1\ \mu s$ was chosen, and $M = 16$ poles were used to approximate the line's frequency-dependent series impedance. The accuracy of the simulated waveforms was confirmed by comparison with a direct frequency-domain solution of the transmission line system. The ability of the method to accurately model the effect of loss and dispersion is evident in the results.

Assuming that the simulator dictates the time step Δt, there are two parameters in the proposed FDTD algorithm whose values should be determined. One is the space step Δx, and the other is the number of poles M. For a specified time step the space step should be chosen as

$$\frac{\Delta x}{\Delta t}\geq v \quad (24)$$

in order to ensure the stability of the algorithm [16]. Here, v is the maximum propagation speed of a signal on the transmission line. For a general lossy line there is no specific propagation speed, but one can choose v to be the speed of light which guarantees that the algorithm is stable for any line. In our examples,

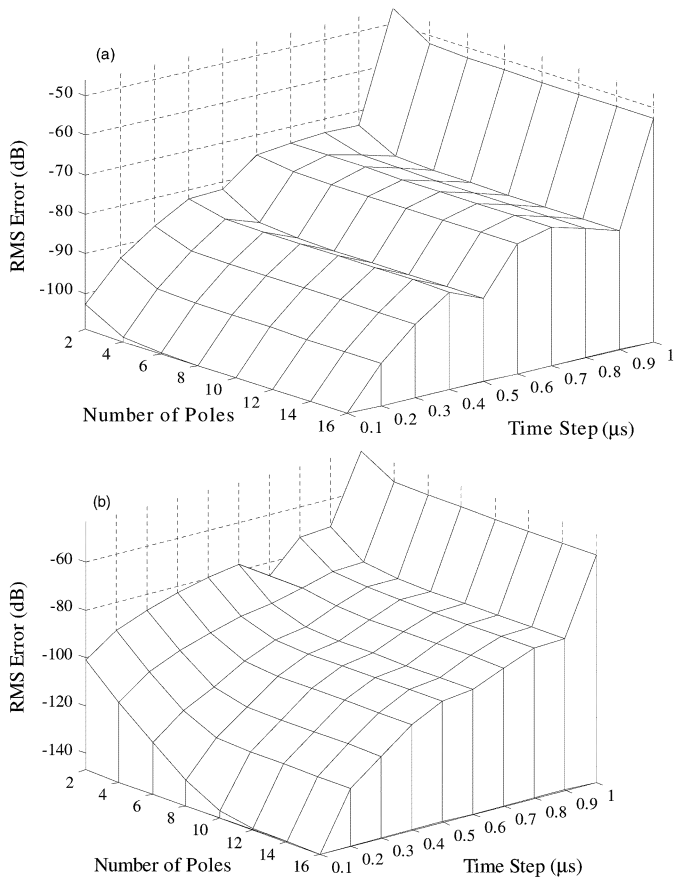

Fig. 8. RMS error of the computed (a) sending end and (b) receiving end voltages of the line for different number of poles and different values of the time step. A frequency-domain solution was used as the reference.

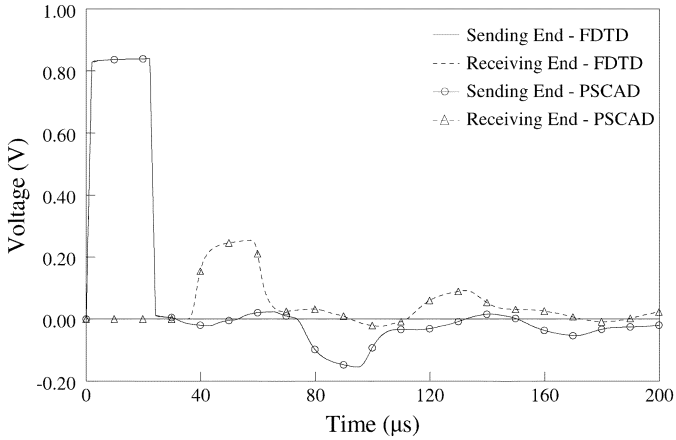

Fig. 9. Terminal voltages of the nonuniform line, when excited by a trapezoidal waveform. FDTD Results are compared to those obtained using PSCAD.

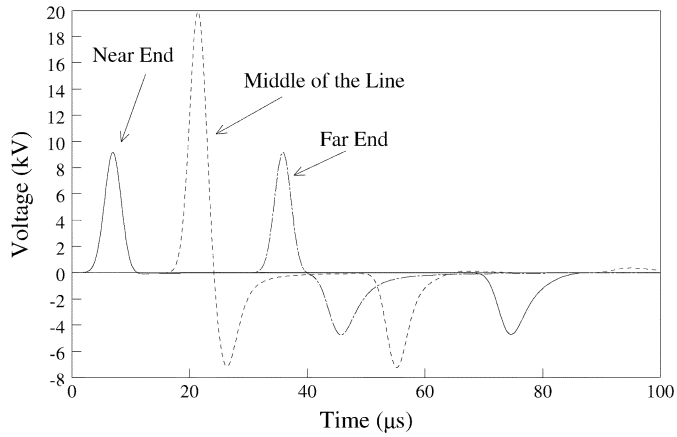

Fig. 10. Induced voltages at the line terminals and at the middle of the line. The line is illuminated by a Gaussian plane wave. The amplitude of the incident electric field is 1 kV/m.

we choose Δx as small as possible, as determined by the lower limit in (24), which minimizes numerical errors.

Fig. 8 shows the RMS difference (over a 200-μs window) between the terminal voltages calculated using FDTD method and those calculated using a frequency-domain method for different values of the time step and number of poles. These results show that the FDTD neither requires a very small time step (as compared to the exciting waveform risetime) nor needs a large number of poles to accurately simulate the frequency-dependent behavior of the transmission line.

B. Nonuniform Transmission Line

One of the advantages of the proposed FDTD method is that it can be used to simulate nonuniform transmission lines, whose electrical characteristics are varying with spatial variable. As an example, we consider the case for which the conductivity of the ground is changing, such as that encountered when a section of the transmission line traverses a body of water. The same line configuration and excitation as the previous example (Table I and Fig. 7) is used, except in this case, the middle 2 km of the line is over water with a resistivity of 0.25 Ωm. The rest of line has a ground resistivity of 10 000 Ωm, as before. The simulated waveforms at the two terminals are plotted in Fig. 9. The results were the same as those obtained using PSCAD with three cascaded frequency-dependent line models. When compared with Fig. 7, the effect of the reflection and increased loss from the section over water is evident.

In general, any desired variation of the line characteristics, including gradual changes, can be implemented with the FDTD approach. We chose a rapid change so that we can confirm the accuracy of the method by comparing with other models.

C. Plane Wave Excitation

We next consider an external plane wave excitation of a transmission line. This could be used to simulate the coupling of a source far from the transmission line. The transmission line is the same as that used in part A, terminated, in this case, with its high frequency surge impedance. The electric field of the incident plane wave has a Gaussian waveform with a peak value of 1 kV/m and 10%–90% risetime of 2.4 μs. The incidence direction, referring to Fig. 6(a), is $\varphi = 30°, \theta = 90°$, and the polarization angle is $\eta = 0°$. The induced voltages at the two terminals of the line, as well as the mid point of the line are plotted in Fig. 10.

D. Nearby Lightning Stroke

Nearby lightning strokes can generate a high transient voltage on transmission lines. As shown in Fig. 6(b), we model the

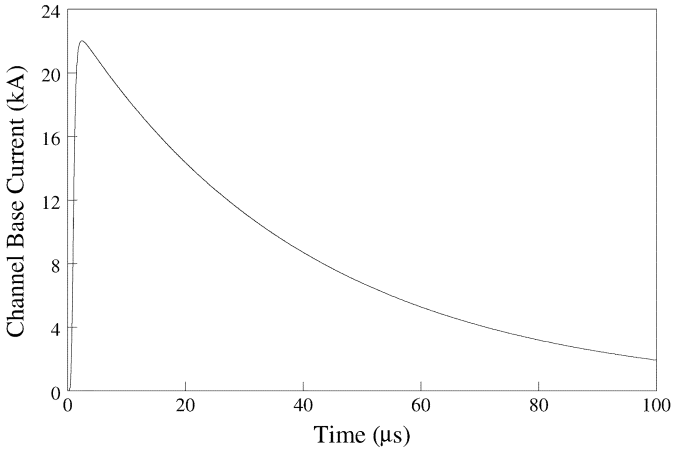

Fig. 11. Channel-base current generated using the Heidler formulation [27]. The peak value of this waveform is 22 kA, and it has a 10%–90% risetime of 0.8 μs, and a 29.6 μs half- magnitude width.

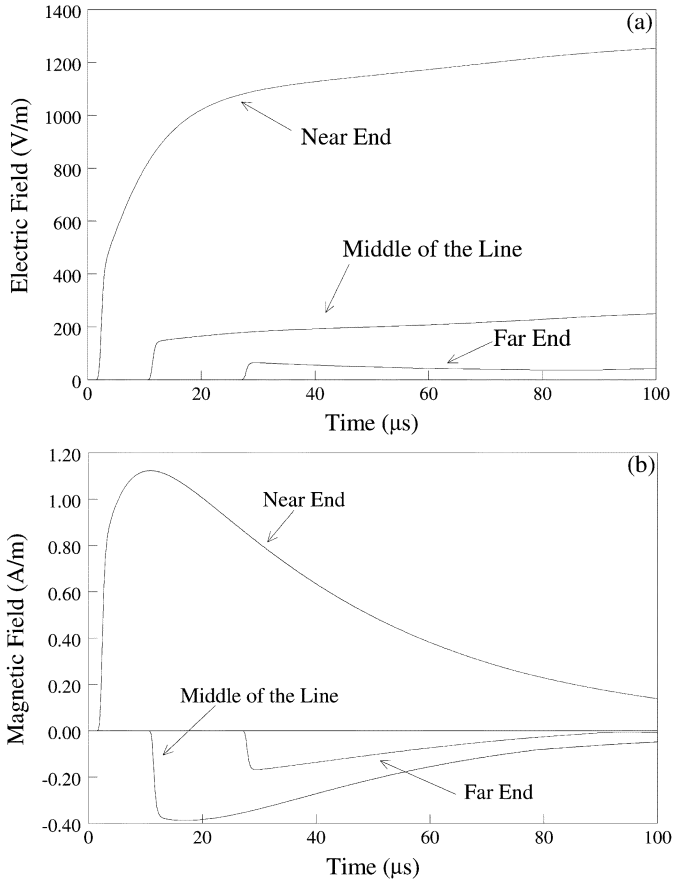

Fig. 12. Transverse electric field (a) and the normal magnetic field (b) along the line, generated by the lightning return-stroke channel. Note that when $x > x_0$ [see Fig. 6(b)], the polarity of the magnetic field is inverted.

lightning return stroke channel as a monopole antenna that radiates electromagnetic fields into the free space. The Modified Transmission Line Linear (MTLL) model was chosen for the return stroke channel, which assumes that the current wave is linearly attenuated as it travels along the lightning channel [26]. A channel-base current, with a peak value of 22 kA, a 10%–90% risetime of 0.8 μs, and a 29.6 μs half-magnitude width, is chosen for this example, as shown in Fig. 11. We have used Heidler formulation [27] for generating this waveform. Once the current distribution along the channel is determined, the formulation presented in [28] is used to calculate the transverse component of electric field and normal component of magnetic field along the line. In Fig. 12, the electromagnetic fields at the two ends of the line, as well as the middle point, are plotted assuming the location of the lightning return stroke channel to be at point ($x_0 = 1000$ m, $y_0 = 1000$ m). Fig. 12 indicates the near-field nature of the electromagnetic fields and how their waveforms change as a function of distance from the source [26], [28]. Finally, the induced voltages at the two terminals and at the middle of the line are plotted in Fig. 13.

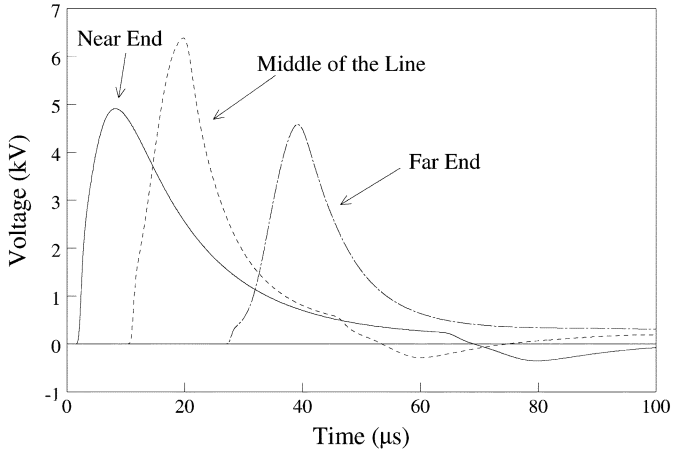

Fig. 13. Induced transient voltages caused by a nearby lightning stroke. The current waveform of the return stroke channel is shown in Fig. 11.

IV. Conclusion

In this paper, a circuit model for integrating a lossy dispersive transmission line within a circuit simulator was presented. This model is based on a time-domain finite-difference solution of the transmission-line equations. Each conductor of the line is modeled as a two-port stamp, which only includes resistive elements and dependent current sources. This makes the scheme independent from the method used for solving the differential equations by the circuit simulator. The model is amenable to simulating both nonuniform lines and external excitation sources.

References

[1] F. H. Branin Jr., "Transient analysis of lossless transmission lines," *Proc. IEEE*, vol. 55, no. 11, pp. 2012–2013, Nov. 1967.

[2] A. Budner, "Introduction of frequency-dependent line parameters into an electromagnetic transient program," *IEEE Trans. Power App. Syst.*, vol. PAS-89, no. 1, pp. 88–97, Jan. 1970.

[3] J. K. Snelson, "Propagation of traveling waves on transmission lines-frequency dependent parameters," *IEEE Trans. Power App. Syst.*, vol. PAS-91, pp. 85–91, Jan./Feb. 1972.

[4] J. R. Marti, "Accurate modeling of frequency-dependent transmission lines in electromagnetic transient simulations," *IEEE Trans. Power App. Syst.*, vol. PAS-101, no. 1, pp. 147–155, Jan. 1982.

[5] *PSCAD User's Manual*. Winnipeg, MB, Canada: HVDC Res. Center, 2003.

[6] *Electromagnetic Transient Program (EMTP) Rule Book*. Portland, OR: Bonneville Power Admin., 1984.

[7] B. Gustavsen, G. Irwin, R. Mangelrod, D. Brandt, and K. Kent, "Transmission line models for the simulation of interaction phenomena between parallel AC and DC overhead lines," in *Proc. Int. Conf. Power Syst. Transients*, Budapest, Hungary, Jun. 20–24, 1999, pp. 61–67.

[8] L. Marti, "Simulation of transients in underground cables with frequency-dependent modal transformation matrices," *IEEE Trans. Power Del.*, vol. 3, no. 3, pp. 1099–1110, Jul. 1988.
[9] B. Gustavsen and A. Semlyen, "Simulation of transmission line transients using vector fitting and modal decomposition," *IEEE Trans. Power Del.*, vol. 13, no. 2, pp. 605–614, Apr. 1998.
[10] T. Noda, N. Nagaoka, and A. Ametani, "Phase domain modeling of frequency-dependent transmission lines by means of an ARMA model," *IEEE Trans. Power Del.*, vol. 11, no. 1, pp. 401–411, Jan. 1996.
[11] F. Castellanos and J. R. Marti, "Full frequency-dependent phase-domain transmission line model," *IEEE Trans. Power Syst.*, vol. 12, no. 3, pp. 1331–1339, Aug. 1997.
[12] B. Gustavsen and A. Semlyen, "Calculation of transmission line transients using polar decomposition," *IEEE Trans. Power Del.*, vol. 13, no. 3, pp. 855–862, Jul. 1998.
[13] A. Morched, B. Gustavsen, and M. Tartibi, "A universal line model for accurate calculation of electromagnetic transients on overhead lines and underground cables," *IEEE Trans. Power Del.*, vol. 14, no. 3, pp. 1032–1038, Jul. 1999.
[14] A. K. Agrawal, H. J. Price, and S. H. Gurbaxani, "Transient response of multiconductor transmission lines excited by a nonuniform electromagnetic field," *IEEE Trans. Electromagn. Compat.*, vol. EMC-22, no. 2, pp. 119–129, May 1980.
[15] A. R. Djordjevic, T. S. Sarkar, and R. F. Harrington, "Time domain response of multiconductor transmission lines," *Proc. IEEE*, vol. 75, no. 6, pp. 743–764, Jun. 1987.
[16] C. R. Paul, *Analysis of Multiconductor Transmission Lines*. New York: Wiley, 1994, ch. 5.
[17] A. Orlandi and C. R. Paul, "FDTD analysis of lossy multiconductor transmission lines terminated in arbitrary loads," *IEEE Trans. Electromagn. Compat.*, vol. 38, no. 3, pp. 388–399, Aug. 1996.
[18] G. Antonini, A. Orlandi, and C. R. Paul, "An improved method of modeling lossy transmission lines in finite-difference time-domain analysis," in *Proc. IEEE Int. Symp. Electromagn. Compat.*, vol. 1, Seattle, WA, Aug. 2–6, 1999, pp. 435–439.
[19] D. Mardare and J. LoVetri, "The finite-difference time-domain solution of lossy MTL networks with nonlinear junctions," *IEEE Trans. Electromagn. Compat.*, vol. 37, no. 2, pp. 252–259, May 1995.
[20] B. Gustavsen and A. Semlyen, "Rational approximation of frequency-domain responses by vector fitting," *IEEE Trans. Power Del.*, vol. 14, no. 3, pp. 1052–1061, Jul. 1999.
[21] K. S. Kunz and R. J. Luebbers, *The Finite Difference Time Domain Method in Electromagnetics*. Boca Raton, FL: CRC, 1993.
[22] J. R. Carson, "Wave propagation in overhead wires with ground return," *Bell Syst. Tech. J.*, vol. 5, pp. 539–554, 1926.
[23] F. B. Hildebrand, *Introduction to Numerical Analysis*, Second ed. New York: Dover, 1987, ch. 9, p. 457.
[24] J. A. Roden, C. R. Paul, W. T. Smith, and S. D. Gedney, "Finite-difference time-domain analysis of lossy transmission lines," *IEEE Trans. Electromagn. Compat.*, vol. 38, no. 1, pp. 15–24, Feb. 1996.
[25] C. D. Taylor, R. S. Satterwhite, and C. W. Harrison, "The response of a terminated two-wire transmission line excited by a nonuniform electromagnetic field," *IEEE Trans. Antennas Propagat.*, vol. AP-13, pp. 987–989, 1965.
[26] V. A. Rakov and M. A. Uman, "Review and evaluation of lightning return stroke models including some aspects of their application," *IEEE Trans. Electromagn. Compat.*, vol. 40, no. 4, pp. 403–426, Nov. 1998.
[27] F. Heidler, J. M. Cvetić, and B. V. Stanić, "Calculation of lightning current parameters," *IEEE Trans. Power Del.*, vol. 14, no. 2, pp. 399–404, Apr. 1999.
[28] M. J. Master and M. A. Uman, "Transient electric and magnetic fields associated with establishing a finite electrostatic dipole," *Amer. J. Phys.*, vol. 51, pp. 118–126, 1983.

Behzad Kordi received the B.Sc. (with distinction), M.Sc., and Ph.D. degrees, all in electrical engineering, from Amirkabir University of Technology (Tehran Polytechnic), Tehran, Iran, in 1992, 1995, and 2000, respectively.

During 1998 and 1999, he was with the Lightning Studies Group at the University of Toronto, Toronto, ON, Canada, from which he was awarded a Graduate Research Grant by the Electrical and Computer Engineering Department. In 2002, he joined the Electrical and Computer Engineering Department, University of Manitoba, Winnipeg, MB, Canada, as a Post Doctoral Fellow, where he has recently become an Assistant Professor. His research interests concern computational electromagnetics, electromagnetic compatibility (EMC), time-domain simulation of interconnects and transmission lines, and electromagnetic probes. He is the author/coauthor of more than 20 scientific papers published in reviewed journals or presented at international conferences.

Joe LoVetri (M'91) was born in Enna, Italy, in 1963. He received the B.Sc. (with distinction) and M.Sc. degrees, both in electrical engineering, from the University of Manitoba, Winnipeg. MB, Canada, in 1984 and 1987, respectively. He received the Ph.D. degree in electrical engineering from the University of Ottawa, Ottawa, ON, Canada, in 1991.

From 1984 to 1986, he was EMI/EMC engineer at Sperry Defence Division, Winnipeg. From 1986 to 1988, he was TEMPEST engineer at the Communications Security Establishment, Ottawa. From 1988 to 1991, he was a Research Officer with the Institute for Information Technology, National Research Council of Canada, Ottawa. From 1991 to 1999, he was an Associate Professor with the Department of Electrical and Computer Engineering, The University of Western Ontario, London, ON, Canada. During 1997 and 1998, he spent a sabbatical year at the TNO Physics and Electronics Laboratory in The Netherlands. He is currently a Professor with the Department of Electrical and Computer Engineering, University of Manitoba. His main interests lie in time domain computational electromagnetics, modeling of electromagnetic compatibility problems, ground-penetrating RADAR, and wideband identification techniques.

Greg E. Bridges (M'82–SM'04) received the B.Sc., M.Sc., and Ph.D. degrees in electrical engineering from the University of Manitoba, Winnipeg, MB, Canada, in 1982, 1984, and 1989, respectively.

He joined the Department of Electrical and Computer Engineering, University of Manitoba, in 1989, where he is currently a Professor. In 1996, he was a visiting scientist at the Communications Research Centre, Ottawa, ON, Canada. He is currently the Principle Researcher for the Advanced RF Test Lab., National Microelectronics and Photonics Test Collaboratory, Canada. He has authored or coauthored publications in the areas of computational electromagnetics and microwave measurement techniques, and he holds several patents related to RFIC probing. His research involves computational electromagnetics and the development of nanoprobe-based measurement techniques for high-frequency microelectronics test and failure analysis.